distribution of E values, and subsequently confirmed by the absence of crystallographic mirror-plane symmetry perpendicular to the b axis (although the molecule itself possesses two obvious, potential mirror planes). All non-hydrogen atoms were refined as in **1**. Hydrogen atoms were ignored.

Acknowledgment for financial support is made to the Air Force Office of Scientific Research, Air Force Systems Command, USAF (Grant No. AFOSR-88-0273), and to Chevron Research Co. The U.S. Government is authorized to reproduce and distribute reprints for Governmental purposes. T.D.T. thanks the Alfred P. Sloan Foundation for a research fellowship (1988-90).

Supplementary Material Available: Tables of crystallographic data, bond distances and angles, anisotropic temperature factors, and hydrogen atom coordinates (13 pages); listings of calculated and observed structure factors (43 pages). Ordering information is given on any current masthead page.

Contribution from the Department de Química Inorgànica, Facultat de Ciències Químiques de la Universitat de València, 46100 Burjassot (València), Spain, Departament de Cristal.lografia, Mineralogia i Dipòsits Minerals, Universitat de Barcelona, Barcelona, Spain, Laboratoire de Chimie Inorganique, CNRS URA 420, Université de Paris-Sud, 91405 Orsay, France, and Laboratoire de Chimie Biorganique and Bioinorganique CNRS URA 1384, Université de Paris-Sud, 91405 Orsay, France

Synthesis and Magnetic Properties of Binuclear Iron(III) Complexes with Oxalate, 2,5-Dihydroxy-1,4-benzoquinone Dianion, and Squarate as Bridging Ligands. Crystal Structure of (μ-1,3-Squarato)bis[(N,N'-ethylenebis(salicylideneaminato))(methanol)iron(III)]

Francesc Lloret,[1a] Miguel Julve,*[1a] Juan Faus,[1a] Xavier Solans,[1b] Yves Journaux,*[1c] and Irène Morgenstern-Badarau[1d]

Received February 16, 1989

Three iron(III) complexes of formulas $[Fe_2(salen)_2ox]\cdot H_2O$ (**1**), $[Fe_2(salen)_2dhbq]\cdot 1.5H_2O$ (**2**), and $[Fe_2(salen)_2(CH_3OH)_2sq]$ (**3**), where salen = N,N'-ethylenebis(salicylideneaminate) ($C_{16}H_{14}N_2O_2^{2-}$), ox = oxalate ($C_2O_4^{2-}$), dhbq = the dianion of 2,5-dihydroxy-1,4-benzoquinone ($C_6H_2O_4^{2-}$), and sq = the dianion of 3,4-dihydroxy-3-cyclobutene-1,2-dione ($C_4O_4^{2-}$), have been prepared. The crystal structure of **3** has been solved at room temperature. It crystallizes in the monoclinic system, space group $P2_1/a$, with a = 13.278 (3) Å, b = 14.464 (3) Å, c = 9.574 (2) Å, β = 96.24 (2)°, and Z = 2. The structure consists of μ-1,3-squarato-bridged [Fe^{III}(salen)CH_3OH)] binuclear units. The iron(III) is hexacoordinate, with the four donor atoms of salen and two oxygen atoms, one of a methanol molecule and the other of the squarate bridge, building a distorted octahedron around the metal ion. The magnetic behavior of all three complexes has been studied in the 4.2-300 K temperature range. The HDVV, ($\hat{H} = -J\hat{S}_1\cdot\hat{S}_2$), $S_1 = S_2 = {}^5/_2$ spin-exchange model applied to the measured magnetic susceptibilities vs temperature yields J values of -7.1, -0.92, and -0.39 cm^{-1} for **1-3**, respectively. A discussion about the pathway of exchange interaction in this series is presented.

Introduction

It is now well-known that magnetic interactions between paramagnetic centers can be propagated not only by single-atom but also by multiatom bridges.[2] The distance dependence of the magnetic coupling is of continuing interest[3] although, up to now, most of the reported results have dealt with binuclear copper(II) complexes with intramolecular copper-copper distances in the range 5-8 Å; relatively strong interactions were observed with bridging ligands such as end-to-end azide,[4] oxalate,[5] oxamate and oxamide,[3,6] dithiooxalate,[7] tetrathiooxalate,[8] derivatives of the dianion of 2,5-dihydroxy-1,4-benzoquinone,[9] and 2,2'-bipyrimidine.[10]

Intramolecular copper-copper distances greater than 10 Å were achieved with bridging ligands such as terephthalate[11] and 4,4'-bipyridine,[12] and weak antiferromagnetic interactions were observed in both cases. In fact, it is most likely that in the former case the interaction is intermolecular instead of intramolecular, whereas in the latter the observed antiferromagnetic coupling cannot be attributed to intermolecular interaction only. These two examples illustrate the difficulties involved in the determination of the limit of intramolecular exchange interaction through extended bridges. The distance-dependent limit to exchange coupling was raised by Coffman and Buettner.[13] The question

(1) (a) Universitat de València. (b) Universitat de Barcelona. (c) Laboratoire de Chimie Inorganique, Université de Paris-Sud. (d) Laboratoire de Chimie Biorganique and Bioinorganique, Université de Paris-Sud.
(2) Willett, R. D., Gatteschi, D., Kahn, O., Eds. *Magneto-Structural Correlations in Exchange Coupled Systems*; Reidel: Dordrecht, Holland, 1985.
(3) See, e.g.: Hendrickson, D. N. In ref 2, p 523 ff.
(4) Agnus, Y.; Louis, R.; Weiss, R. *J Am. Chem. Soc.* **1979**, *101*, 3381.
(5) (a) Felthouse, T. R.; Laskowski, E. J.; Hendrickson, D. N. *Inorg. Chem.* **1977**, *16*, 1077. (b) Julve, M.; Verdaguer, M.; Kahn, O.; Gleizes, A.; Philoche-Levisalles, M. *Inorg. Chem.* **1983**, *22*, 358. (c) *Inorg. Chem.* **1984**, *23*, 3808. (d) Julve, M.; Faus, J.; Verdaguer, M.; Gleizes, A. *J. Am. Chem. Soc.* **1984**, *106*, 8306.
(6) (a) Verdaguer, M.; Kahn, O.; Julve, M.; Gleizes, A. *Nouv. J. Chim.* **1985**, *9*, 325. (b) Nonoyama, K.; Ojima, H.; Ohki, K.; Nonoyama, M. *Inorg. Chim. Acta* **1980**, *41*, 155. (c) Bencini, A.; Benelli, C.; Gatteschi, D.; Zanchini, C.; Fabretti, A. C.; Franchini, G. C. *Inorg. Chim. Acta* **1984**, *86*, 169. (d) Journaux, Y.; Sletten, J.; Kahn, O. *Inorg. Chem.* **1985**, *24*, 4063.
(7) (a) Girerd, J. J.; Jeannin, S.; Jeannin, Y.; Kahn, O. *Inorg. Chem.* **1978**, *17*, 3034. (b) Chauvel, C.; Girerd, J. J.; Jeannin, Y.; Kahn, O.; Lavigne, G. *Inorg. Chem.* **1979**, *18*, 3015. (c) Girerd, J. J.; Kahn, O. *Angew. Chem., Suppl.* **1982**, 953. (d) Veit, R.; Girerd, J. J.; Kahn, O.; Robert, F.; Jeanin, Y.; El Murr, N. *Inorg. Chem.* **1984**, *23*, 4448.
(8) Vicente, R.; Ribas, J.; Alvarez, S.; Solans, X.; Fontaltaba, M.; Verdaguer, M. *Inorg. Chem.* **1987**, *26*, 4004.
(9) Tinti, F.; Verdaguer, M.; Kahn, O.; Savariault, J. M. *Inorg. Chem.* **1987**, *26*, 2380.
(10) (a) Julve, M.; De Munno, G.; Bruno, G.; Verdaguer, M. *J. Chem. Res., Synop.* **1987**, 152. (b) *Inorg. Chem.* **1988**, *27*, 3160.
(11) Verdaguer, M.; Gouteron, J.; Jeannin, S.; Kahn, O. *Inorg. Chem.* **1984**, *23*, 4291.
(12) Julve, M.; Verdaguer, M.; Faus, J.; Tinti, F.; Moratal, J.; Monge, A.; Gutiérrez-Puebla, E. *Inorg. Chem.* **1987**, *26*, 3520.
(13) Coffman, R. E.; Buettner, G. R. *J. Phys. Chem.* **1979**, *83*, 2387.

0020-1669/90/1329-2232$02.50/0

Table I. Crystallographic Data for **3**

chem formula	$C_{38}H_{36}N_4Fe_2O_{10}$	space group	$P2_1/a$
a, Å	13.278 (3)	T, °C	25
b, Å	14.464 (3)	λ, Å	0.71073
c, Å	9.574 (2)	ρ_{calcd}, g·cm^{-3}	1.487
β, deg	96.24 (2)	μ, cm^{-1}	8.83
V, Å^3	1828 (1)	R^a	0.059
Z	2	$R_w{}^b$	0.068
fw	818.4		

$^a R = \sum||F_o| - |F_c||/\sum|F_o|$. $^b R = [\sum w||F_o| - |F_c||^2/\sum w|F_o|^2]^{1/2}$. The function minimized was $w||F_o| - |F_c||^2$, where $w = [\sigma^2|F_o| + 0.032|F_o|^2]^{-1}$.

at hand is how far two paramagnetic ions can be separated from each other and what requirements of symmetry and energy must fill the extended bridging ligand to lead to an appreciable exchange coupling. The study of such systems could give some insights into the pathways of electron transfer in biological electron-transport chains and improve our understanding of electron transfer in mixed-valence complexes. On the other hand, new polynuclear compounds with predictable magnetic properties can be designed and isolated on the basis of such studies by using so-called "molecular engineering".[5b,14]

In the frame of our work on the interaction between transition-metal ions through extended bridging ligands we focus here on the efficiency of oxalate ($C_2O_4^{2-}$, ox), squarate ($C_4O_4^{2-}$, sq), and 2,5-dihydroxy-1,4-benzoquinone ($C_6H_2O_4^{2-}$, dhbq) dianions to couple two high-spin iron(III) ions. In this paper, we report the synthesis and magnetic properties of three iron(III) binuclear complexes of formulas $[Fe_2(salen)_2ox]\cdot H_2O$ (**1**), $[Fe_2(salen)_2dhbq]\cdot 1.5H_2O$ (**2**), and $[Fe_2(salen)_2(CH_3OH)_2sq]$ (**3**), where salen = *N*,*N*′-ethylenebis(salicylideneaminate) ($C_{16}H_{14}N_2O_2^{2-}$), and we describe the structure of one of them, namely the squarato complex. As far as we know, it is the first time that the crystal structure of an iron(III)–squarato complex is reported.

Experimental Section

Materials. Oxalic acid (H_2ox), squaric acid (H_2sq), hydranilic acid (H_2dhbq), and piperidine (pip), which correspond to ethanedioic acid, 3,4-dihydroxy-3-cyclobutene-1,2-dione, 2,5-dihydroxy-1,4-benzoquinone, and cyclohexylamine, were purchased from Merck and used as received. $Fe(salen)NO_3$ and $[Fe_2(salen)_2ox]\cdot H_2O$ (**1**) were isolated by reported procedures.[15] Elemental analyses (C, H, N) were performed by the Servei de Microanàlisi del CSIC, Barcelona, Spain.

Synthesis. $(Hpip)_2dhbq\cdot H_2O$. This salt was obtained as a red solid when 4×10^{-2} mol of piperidine was added to a solution of 2×10^{-2} mol of H_2dhbq in 50 mL of acetone. The product was filtered out and washed with acetone and ether. Anal. Calcd for $C_{16}H_{28}N_2O_5$: C, 58.54; H, 8.54; N, 8.54. Found: C, 58.82; H, 8.49; N, 8.60.

$[Fe_2(salen)_2dhbq]\cdot 1.5H_2O$ (2). A 0.5×10^{-3} mol sample of $(Hpip)_2dhbq\cdot H_2O$ dissolved in 10 mL of methanol was added to a refluxing methanolic solution (50 mL) of 1×10^{-3} mol of $Fe(salen)NO_3$ with stirring. A red-brown solid appeared, and after the mixture was refluxed for 0.5 h, the product was separated by filtration and washed with methanol and acetone. Anal. Calcd for $C_{38}H_{33}N_4O_{9.5}Fe_2$ (**2**): C, 56.39; H, 4.11; N, 6.92. Found: C, 56.19; H, 4.16; N, 7.00.

$[Fe_2(salen)_2(CH_3OH)_2sq]$ (3). A methanolic solution of 1×10^{-3} mol of $(Hpip)_2sq$, obtained by mixing piperidine and squaric acid in a 2:1 molar ratio, was added to a refluxing methanolic solution of 2×10^{-3} mol of $Fe(salen)NO_3$. The dark red resulting solution was refluxed for 15 min and cooled at room temperature. The violet polycrystalline solid that appeared was removed by filtration, and prismatic brown single crystals of **3** were obtained by slow evaporation of the red methanolic solution. Anal. Calcd for $C_{38}H_{36}N_4O_{10}Fe_2$ (**3**): C, 55.65; H, 4.39; N, 6.83. Found: C, 55.70; H, 4.29; N, 6.78.

Physical Techniques. Infrared spectra were recorded on a Perkin-Elmer 1750 FTIR spectrophotometer as KBr pellets in the 4000–225-cm^{-1} region. Magnetic measurements were carried out in the 4–300 K temperature range with a previously described Faraday-type magnetometer,[16] equipped with a helium continuous-flow cryostat. $HgCo(NCS)_4$ was used as a susceptibility standard. Corrections for the diamagnetism of the complexes were estimated from Pascal constants as -422×10^{-6}, -442×10^{-6}, and -454×10^{-6} cm^3 mol^{-1} for complexes **1**–**3**, respectively.

Table II. Final Atomic Fractional Coordinates[a] and Equivalent Isotropic Displacement Parameters[b] for the Non-Hydrogen Atoms in **3**

atom	x/a	y/b	z/c	B_{eq}, Å^2
Fe	0.11572 (5)	0.25929 (5)	0.42097 (7)	2.98 (4)
O(1)	0.0519 (3)	0.2701 (3)	0.2333 (4)	3.88 (17)
C(1)	0.0532 (4)	0.2131 (4)	0.1257 (6)	3.61 (23)
C(2)	−0.0183 (5)	0.2260 (5)	0.0083 (6)	4.74 (29)
C(3)	−0.0193 (6)	0.1704 (6)	−0.1094 (7)	6.08 (37)
C(4)	0.0495 (6)	0.0978 (6)	−0.1113 (7)	5.98 (37)
C(5)	0.1192 (6)	0.0841 (5)	0.0015 (8)	5.40 (33)
C(6)	0.1237 (4)	0.1395 (4)	0.1214 (6)	3.90 (24)
C(7)	0.2049 (4)	0.1215 (5)	0.2342 (6)	4.14 (26)
N(7)	0.2182 (3)	0.1647 (3)	0.3483 (5)	3.53 (19)
C(8)	0.3083 (4)	0.1441 (6)	0.4478 (7)	4.83 (31)
C(9)	0.2773 (5)	0.1461 (5)	0.5950 (6)	4.37 (27)
N(10)	0.2113 (3)	0.2256 (3)	0.6068 (5)	3.55 (19)
C(10)	0.2116 (4)	0.2681 (4)	0.7249 (6)	3.49 (22)
C(11)	0.1519 (4)	0.3476 (4)	0.7521 (5)	3.38 (22)
C(12)	0.1683 (5)	0.3886 (4)	0.8863 (6)	4.08 (26)
C(13)	0.1158 (5)	0.4658 (5)	0.9198 (6)	4.80 (30)
C(14)	0.0431 (4)	0.5043 (4)	0.8213 (6)	3.95 (26)
C(15)	0.0225 (4)	0.4657 (4)	0.6914 (6)	3.57 (23)
C(16)	0.0755 (3)	0.3855 (3)	0.6518 (5)	3.01 (20)
O(16)	0.0533 (3)	0.3508 (2)	0.5273 (4)	3.41 (16)
O(17)	0.0184 (3)	0.1571 (2)	0.4641 (4)	3.95 (17)
C(17)	0.0106 (4)	0.0692 (4)	0.4831 (5)	3.30 (21)
C(18)	−0.0715 (3)	0.0154 (4)	0.5274 (5)	2.96 (19)
O(18)	−0.3414 (3)	0.4660 (3)	0.5600 (4)	4.09 (18)
O(19)	0.2252 (3)	0.3639 (3)	0.3826 (4)	4.36 (18)
C(19)	0.2744 (7)	0.3713 (7)	0.2610 (9)	6.50 (46)

[a] Estimated standard deviations in the last significant digits are given in parentheses. [b] $B_{eq} = (8\pi^2/3)\sum_i\sum_j U_{ij}a_i^*a_j^*\mathbf{a}_i\mathbf{a}_j$.

Crystallographic Data Collection and Refinement of the Structure of 3. A prismatic crystal of dimensions 0.1 × 0.1 × 0.2 mm was selected and mounted on a Philips PW-1100 four-circle diffractometer. Unit cell parameters were determined from automatic centering of 25 reflections ($4 \le \theta \le 12°$) and refined by least-squares methods. Cell parameters and other relevant details are quoted in Table I. The octants of data collected were $\pm h,k,l$. Of the 3714 collected reflections, only 2213 were considered as measured. From these, 2208 were considered as observed with $I \ge 2.5\sigma(I)$. The estimate of agreement between equivalent reflections is $R_{int}(\pm h,k,0) = 0.032$ (on F). A full-length table containing crystallographic data collection and structure refinement parameters is given as supplementary material (Table SI). Three reflections were measured every 2 h, as orientation and intensity control and significant intensity decay were not observed. Lorentz–polarization but no absorption corrections were made. No extinction correction was carried out. The structure was solved by direct methods using the MULTAN system of computer programs[17] and refined by full-matrix least-squares methods using the SHELX 76 program.[18] f, f', and f'' were taken from ref 19. All hydrogen atoms, except H(O(19)), which was not found, and H(19a), H(19b), and H(19c), which were introduced in calculated positions, were located from a difference synthesis and refined with an overall isotropic temperature factor, while the remaining atoms were refined anisotropically. Final R and R_w factors were 0.059 and 0.068 for all observed reflections. Maximum and minimum peaks in final difference syntheses were 0.4 and −0.4 e Å^{-3}. The final positional parameters for non-hydrogen atoms are listed in Table II whereas anisotropic thermal parameters and final hydrogen coordinates are given in Tables SII and SIII,[20] respectively.

Results and Discussion

Description of the Structure of 3. Compound **3** crystallizes in the monoclinic space group $P2_1/a$ with the crystallographic in-

(14) Kahn, O. *Inorg. Chim. Acta* **1982**, *62*, 3.
(15) Lloret, F.; Julve, M.; Mollar, M.; Castro, I.; Latorre, J.; Faus, J.; Solans, X.; Morgenstern-Badarau, I. *J. Chem. Soc., Dalton Trans.* **1989**, 729.
(16) Verdaguer, M.; Michalowicz, A.; Girerd, J. J.; Alberding, N.; Kahn, O. *Inorg. Chem.* **1980**, *19*, 3271.
(17) Main, P.; Fiske, S. J.; Hull, S. L.; Lessinger, L.; Germain, G.; Declercq, S. P.; Woolfson, M. M. MULTAN84, an automatic system of computer programs for crystal structure determination from X-ray diffraction data. Universities of York, England, and Louvain Belgium, 1984.
(18) Sheldrick, G. M. SHELX76. University of Cambridge, England, 1976.
(19) *International Tables for X-ray Crystallography*; Kynoch Press: Birmingham, England, 1974; Vol. IV, pp 99–100 and 149.
(20) Supplementary material.

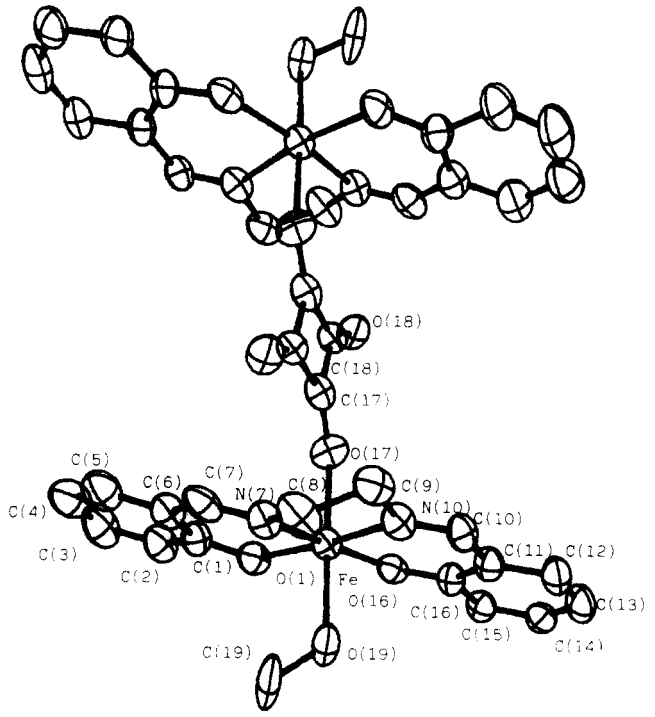

Figure 1. Molecular structure of **3** with atom-labeling scheme. Hydrogen atoms have been omitted for clarity. Thermal ellipsoids are drawn at the 50% probability level.

Table III. Bond Distances (Å) and Angles (deg) for **3**[a]

	Iron Environment		
Fe–O(1)	1.908 (4)	Fe–O(16)	1.913 (3)
Fe–N(7)	2.101 (4)	Fe–O(17)	2.035 (3)
Fe–N(10)	2.127 (4)	Fe–O(19)	2.158 (4)
N(7)–Fe–O(1)	88.8 (2)	O(17)–Fe–N(10)	89.9 (2)
N(10)–Fe–O(1)	166.0 (2)	O(17)–Fe–O(16)	94.2 (1)
N(10)–Fe–N(7)	77.2 (2)	O(19)–Fe–O(1)	91.2 (2)
O(16)–Fe–O(1)	105.7 (1)	O(19)–Fe–N(7)	85.8 (2)
O(16)–Fe–N(7)	163.9 (2)	O(19)–Fe–N(10)	87.2 (2)
O(16)–Fe–N(10)	88.1 (2)	O(19)–Fe–O(16)	86.8 (1)
O(17)–Fe–O(1)	91.3 (2)	O(19)–Fe–O(17)	176.9 (1)
O(17)–Fe–N(7)	94.2 (2)		
	Squarato Bridge		
C(17)–O(17)	1.290 (6)	C(18)–O(18)	1.260 (6)
C(17)–C(18)	1.439 (7)	C(17)–C(18)^{i}	1.476 (7)
C(18)–C(17)–O(17)	130.5 (5)	C(17)–C(18)–O(18)	134.7 (5)
O(17)–C(17)–C(18)^{i}	138.9 (5)	C(17)–C(18)–C(17)^{i}	89.4 (5)
C(18)–C(17)–C(18)^{i}	90.6 (5)	O(18)–C(18)–C(17)^{i}	135.9 (5)

[a] Roman numeral superscript refers to the following symmetry operation: (i) $\bar{x}$, $\bar{y}$, $1 - z$.

version center in the center of the squarate moiety that bridges the two iron–salen entities. An ORTEP[21] view of the molecule and a stereoview of the packing are shown in Figures 1 and 2, respectively. The iron atom is hexacoordinate: two oxygen atoms, one from a methanol molecule and the other from the squarate group, occupy the axial positions of a distorted octahedron around the metal ion, the polyhedron being completed by the quadridentate salen ligand. Selected bond distances and angles are listed in Table III. Whereas the iron–nitrogen bond lengths (2.101 (4) and 2.127 (4) Å) agree well, the iron–oxygen distances vary from 1.908 (4) and 1.913 (3) Å in the salen moiety to 2.158 (4) and 2.035 (3) Å with methanol and squarate ligands, respectively. So, the iron–nitrogen (imine) bond distances are larger than the iron–oxygen (phenolate) ones, as observed in other iron–salen complexes.[22-24] This structural feature is consistent with the greater affinity of iron(III) for phenolate groups. On the other hand, the iron–oxygen (phenolate) distances are nearly equal to the reported ones for the complexes K[Fe(salen)cat][25] and [Fe(salen)PSQ].[25]

This chelating system produces one five-membered and two six-membered metallacycles. The short bond angle around the metal ion in the five-membered ring (the N(7)–Fe–N(10) angle is 77.2 (2)°) causes a sensitive deviation from the ideal 90° value in the O(1)–Fe–O(16) angle (105.7 (1)°) and smaller deviations in the corresponding ones for N(7)–Fe–O(1) and N(10)–Fe–O(16) (88.8 (2) and 88.1 (2)°, respectively). The best equatorial plane is defined by O(1), N(7), N(10), and O(16) atoms of the salen ligand (largest deviation from the mean plane is 0.050 (6) Å for N(7)); the iron is 0.072 (3) Å out of this plane.

The salen adopts a stepped conformation[26] exhibiting values for α, β, and γ of 20.6, 19.8, and 4.6°, respectively. The only other salen complexes with this conformation are the binuclear complexes $[Fe(salen)Cl]_2$[23] and $[Fe_2(salen)_2hq]$,[24] where the iron atom is hexa- and pentacoordinate, respectively. Simple models show that, with the metal in the plane of the four donor salen heteroatoms, the stepped geometry is favored, at least partially because of the gauche conformation of the ethylenediamine group. A near-gauche conformation of the C(8)–C(9) linkage with a torsion angle of −43.2 (8)° is observed in the structure of this complex. The interplanar angle between the salicylidene rings (4.7 (9)°) and the amine torsional angle (177.4 (8)°) agree well with the observed ones (8.4 and 177°) in the pentacoordinate complex $[Fe_2(salen)_2hq]$. The observed bond distances and angles for the salen ligand in **3** are in full agreement with the previously reported ones for other salen-containing iron(III) complexes.

The squarate bridges two iron atoms symmetrically in a 1,3-bismonodentate fashion, and it is planar (largest deviation 0.001 (4) Å). The carbon–oxygen mean bond is slightly larger (1.275 Å) than the mean carbon–oxygen bond in noncoordinated squarate (1.259 Å),[27] while the carbon–carbon mean values are nearly identical (1.458 and 1.456 Å, respectively). These structural features have been observed in other squarate-containing complexes in which the squarate acts as a 1,3-bismonodentate bridge.[28-32] The dihedral angle between the N(7), N(10), O(1), and O(16) mean basal plane and the squarate plane is 85.7 (2)°. The O–C–C angles vary between 130.5 (5) and 139.0 (5)° whereas the C–C–C angles are very close to 90° (90.6 (5) and 89.4 (5)° for C(18)–C(17)–C(18)^{i} and C(17)–C(18)–C(17)^{i}, respectively). The O–C–C angles are close to 135° in all the reported structures where the squarate is not chelating. However, values of the O–C–C angles ranging from 128 to 132° and from 138 to 141° inside and outside the chelate rings, respectively, have been reported for calcium, strontium, and cerium compounds that contain chelating squarates[33].

The iron–iron intramolecular separation is 7.825 (3) Å whereas the shorter iron–iron intermolecular distance is 6.644 (3) Å.

Infrared Spectra. IR spectra of the three herein reported iron complexes exhibit bands due to C–O stretching vibrations in the 1800–1200-cm^{-1} region. As far as the oxalato complex is con-

(21) Johnson, C. K. ORTEP. Report ORNL-3794; Oak Ridge National Laboratory: Oak Ridge, TN, 1965.

(22) Gerloch, M.; Mabbs, F. E. *J. Chem. Soc. A* **1967**, 1900.
(23) Gerloch, M.; McKenzie, E. D.; Towl, A. D. C. *J. Chem. Soc. A* **1969**, 2850.
(24) Heistand, R. H., II; Roe, A. L.; Que, L., Jr. *Inorg. Chem.* **1982**, *21*, 676.
(25) Lauffer, R. B.; Heistand, R. H., II; Que, L., Jr. *Inorg. Chem.* **1983**, *22*, 50.
(26) Calligaris, M.; Nardin, G.; Randaccio, L. *Coord. Chem. Rev.* **1972**, *7*, 385.
(27) MacIntyre, W. M.; Werkema, M. S. *J. Chem. Phys.* **1964**, *42*, 3563.
(28) Van Ooijen, J. A. C.; Reedijk, J.; Spek, A. L. *Inorg. Chem.* **1979**, *18*, 1184.
(29) Weiss, A.; Riegler, E.; Alt, I.; Robl, C. *Z. Naturforsch.* **1986**, *41B*, 18.
(30) Robl, C.; Weiss, A. *Z. Naturforsch.* **1986**, *41B*, 1341.
(31) Petit, J. F.; Trombe, J. C.; Gleizes, A.; Galy, J. *C. R. Acad. Sci., Ser. 2* **1987**, *304*, 1117.
(32) Solans, X.; Aguiló, M.; Gleizes, A.; Faus, J.; Julve, M.; Verdaguer, M. *Inorg. Chem.* **1990**, *29*, 775.
(33) (a) Robl, C.; Weiss, A. *Z. Naturforsch.* **1986**, *41B*, 1490. (b) Robl, C.; Gnutzmann, V.; Weiss, A. *Z. Anorg. Allg. Chem.* **1987**, *549*, 187. (c) Robl, C.; Weiss, A. *Mater. Res. Bull.* **1987**, *22*, 373. (d) Trombe, J. C.; Petit, J. F.; Gleizes, A. *New J. Chem.* **1988**, *12*, 197.

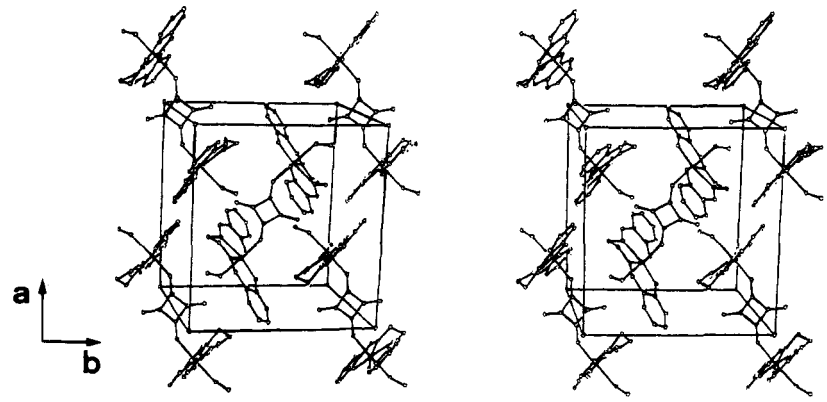

Figure 2. Stereoscopic view of 3.

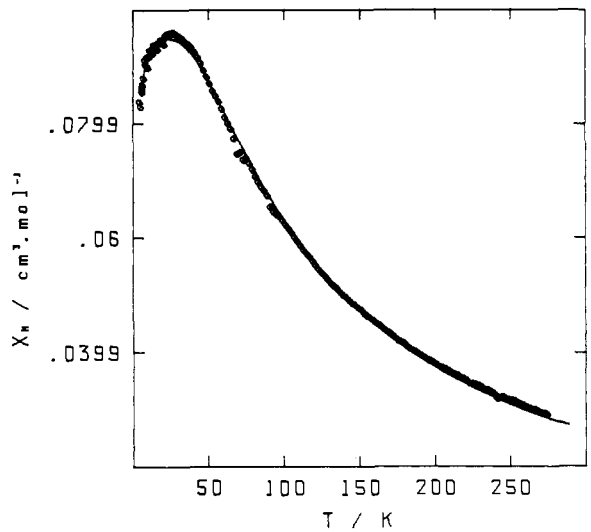

Figure 3. Thermal variation of the molar susceptibility for complex 1 in the form χ_M versus T: (open points) experimental results; (solid line) theoretical fit to eq 4.

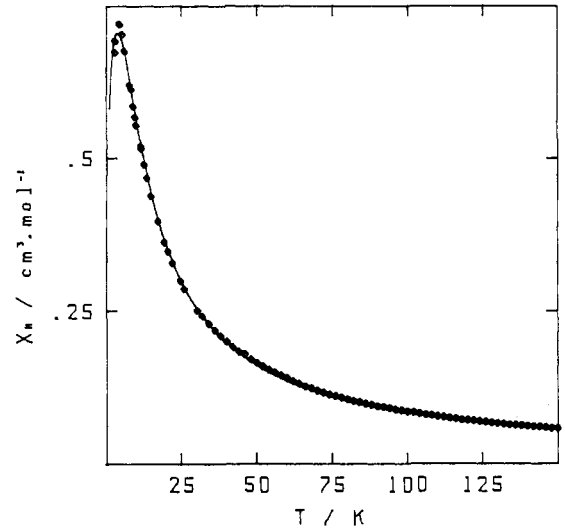

Figure 4. Thermal variation of the molar susceptibility for complex 2 in the form χ_M versus T: (open points) experimental results; (solid line) theoretical fit to eq 4.

cerned, the positions of these bands (1665 (vs) and 1340 (m) cm^{-1}) strongly suggest a bridging bisbidentate coordination mode.[15] Only two C–O stretching bands are observed in the IR spectra of complex **2** at 1540 (vs) and 1385 (s) cm^{-1}, which are attributable to the benzoquinone ligand. The first carbonyl absorption of the dhbq group in the polymeric $[Fe(dhbq)(pyr)]_n$ is centered at ca. 1540 cm^{-1}, and a bisbidentate character was assigned to the dhbq in this compound.[34] On the other hand, H_2dhbq displays carbonyl stretching frequencies at ca. 1650 cm^{-1} and $(Hpip)_2dhbq \cdot H_2O$ exhibits a broad C–O stretching band between 1700 and 1340 cm^{-1}. These facts support the presence of a bisbidentate bridging benzoquinone ligand in **2**. The magnetic properties of **1** and **2** (vide infra) are consistent with this bisbidentate coordination mode of oxalate and benzoquinone ligands. Finally, complex **3** exhibits C–O stretching vibrations of the squarate at 1780 (w) and 1480 (vs) cm^{-1}. The strong shift of this last vibration, when compared to the corresponding one in $K_2C_4O_4$,[35] suggests that the symmetry of the C–O parts of the molecule is lower than D_{4h}, as shown by the above reported X-ray structure.

Magnetic Properties and Exchange Mechanism. The molar magnetic susceptibility, χ_M, versus temperature plots for **1** and **2** are shown in Figures 3 and 4, respectively. For complex **3** the results are given in Figure 5 under the form of the $\chi_M T$ versus T plot. As the temperature decreases, χ_M increases much more slowly than expected for a Curie law in all three complexes. χ_M reaches a maximum around 26.8 K (χ_M = 0.096 cm^3 mol^{-1}) and 4 K (χ_M = 0.707 cm^3 mol^{-1}) for **1** and **2**, respectively. This behavior is characteristic of an antiferromagnetic coupling leading

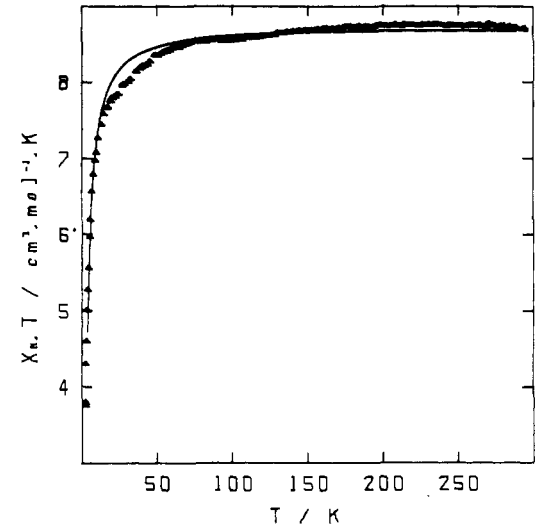

Figure 5. Thermal variation of the molar susceptibility for complex 3 in the form $\chi_M T$ versus T: (open points) experimental results; (solid line) theoretical fit to eq 4.

to a singlet ground state. No maximum is observed for **3**, and χ_M increases continuously with decreasing temperature. Nevertheless, the $\chi_M T$ plot reveals a large deviation from the Curie law.

Compounds **2** and **3** are EPR silent. The X-band spectrum of **1** at 4.2 K exhibits a prominent and broad unresolved feature around $g = 2$ and a weak one at $g = 4$, revealing that in such a complex $D < h\nu$ for at least one of the low-lying spin states. These

(34) Wrobleski, J. T.; Brown, D. B. *Inorg. Chem.* **1979**, *18*, 498.
(35) Ito, M.; West, R. *J. Am. Chem. Soc.* **1963**, *85*, 2580.

Table IV. Best Fitted Values for J and g in **1–3**

compd	$-J$, cm^{-1}	g	ρ, %	10^4R^a
1	7.1	2.02	2.6	1.1
2	0.92	2.00	0	2.3
3	0.39	2.00	0	1.5

^{a} R is the agreement factor defined as $R = \sum_i((\chi_{obsd})_i - (\chi_{theor})_i)^2/\sum_i(\chi_{obsd})_i^2$ for **1** and **2** and as $R = \sum_i((\chi T_{obsd})_i - (\chi T_{theor})_i)^2/\sum_i(\chi T_{obsd})_i^2$ for **3**.

facts clearly indicate that exchange interaction is operative in **1–3**, leading to spin states with integer spin values.

To fit quantitatively the magnetic data, we first consider the exchange interaction as the leading term with the corresponding spin Hamiltonian

$$\hat{H} = -J\hat{S}_1\cdot\hat{S}_2 \tag{1}$$

in which $S_1 = S_2 = {}^5/_2$. Then, the Zeeman interaction is taken into account as an effective spin Hamiltonian associated with each exchange energy level

$$\hat{H}' = g\beta H(\hat{S}_1 + \hat{S}_2) \tag{2}$$

We assume an isotropic and identical g factor for all these levels. All fine-structure effects have been neglected. The derived susceptibility equation is obtained as

$$\chi_D = \left(\frac{2N\beta^2g^2}{kT}\right)\frac{x + 5x^3 + 14x^6 + 30x^{10} + 55x^{15}}{1 + 3x + 5x^3 + 7x^6 + 9x^{10} + 11x^{15}} \tag{3}$$

with $x = \exp(J/kT)$. In order to take into account the presence of uncoupled impurity, we expressed the observed susceptibility as

$$\chi_M = \chi_D(1 - \rho) + \chi_I\rho \tag{4}$$

χ_I was assumed to be for a monomeric high-spin Fe(III) compound of the same molecular weight as one corresponding to complex **1**, **2**, or **3** with a magnetic susceptibility obeying a Curie law

$$\chi_I = 35N\beta^2g^2/12kT \tag{5}$$

The results of the fit are summarized in Table IV. Excellent theory–experiment agreement has been obtained for complexes **1–3**. Identical J and g values are obtained for **1** with $\rho = 0$, but the maximum of susceptibility is not well fitted, leading to a somewhat higher R value. In the case of **1**, the exchange parameter value obtained from the fit can be considered as an accurate result. Indeed, the order of magnitude of the D parameter suggested by EPR ($D < h\nu$) leads to $D \ll J$ and justifies the consideration of the exchange phenomenon as the leading term. The weak interaction found in the case of **2** and **3** might be considered not as accurately as the one found in **1** because a phenomenon of the same order of magnitude, the fine-structure effect, has been neglected (the complex being EPR silent; at least, $D > h\nu$). Then the exchange parameter value has to be taken as an upper limit of the magnitude of the exchange interaction. Nevertheless, the presence of a maximum of χ_M for **2** (Figure 4) indicates that exchange interaction is the most important interaction in such a complex, leading to a singlet ground state.

To the best of our knowledge, only two examples in the literature illustrated the efficiency of the oxalate ligand to couple two high-spin iron(III) ions, $[Fe_2(acac)_4ox]\cdot{}^1/_2\ H_2O$[36] and $[Fe_2(phen)_4ox]Cl_4$,[37] with J values of −7.22 and −6.8 cm^{-1}, respectively. Both are nearly identical with the one reported herein. In spite of an Fe···Fe separation greater than 5 Å, this interaction is of the same order of magnitude as the one occurring in bis(μ-hydroxo)binuclear Fe(III) complexes with an Fe···Fe distance of about 3 Å.[38]

It is well-known that the bisbidentate oxalate ligand is particularly able to propagate the electronic effects when the xy exchange pathway is operative.

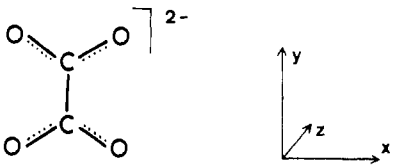

The strong overlap between the xy-type magnetic orbitals centered on the metal ions and delocalized toward the oxygen atoms of the oxalate bridge[39] leads to a large antiferromagnetic coupling. Such a situation occurs in (μ-oxalato)copper(II)[5] and (μ-oxalato)-nickel(II)[40] binuclear complexes. The special efficiency of Cu(II) to yield antiferromagnetic interactions compared to Fe(III) is easily evidenced when J values for (μ-oxalato)copper(II) and (μ-oxalato)iron(III) binuclear species are compared. To deal with comparable values, we take into account the number of unpaired electrons on each magnetic center (1 for copper(II) and 5 for iron(III)) and we compare the n^2J values.[41] We have

$$\underset{385.4\ \text{cm}^{-1}}{J_{Cu\text{-}Cu}} > \underset{175\ \text{cm}^{-1}}{J_{Fe\text{-}Fe}}$$

These values[42] demonstrate that the interaction in the binuclear Cu(II) complex is more efficient than the expected one for the binuclear Fe(III) complex, everything being equal. In molecular orbital terms, the orbital of the bridging oxalate interacts with the metal orbitals that contain the unpaired electrons. The stronger the interaction, the stronger the antiferromagnetic coupling is. Two main parameters govern this interaction: (i) the overlap between the 3d orbitals and the bridge symmetry-adapted molecular orbitals and (ii) the energy difference between these orbitals.

For these two parameters one can expect a smaller interaction when substituting Cu(II) by Fe(III) ions. The iron(III)–oxygen (oxalate) distances are longer than the corresponding Cu(II) distances.[15] In other words, the overlap between the 3d orbitals and the bridge orbital is smaller for Fe(III) than for Cu(II). This leads to a larger spin delocalization on the bridge and a greater J value for the xy pathway in the Cu(II) binuclear compound. Although a π pathway involving $3d_{xz}$ and $3d_{yz}$ magnetic orbitals could be expected for the Fe(III) binuclear compound, its contribution is extremely small owing to the fact that the $3d_{xz}$ and $3d_{yz}$ magnetic orbitals do not point toward the oxalate oxygen atoms. This leads to a small overlap between the symmetry-adapted oxalate π orbitals and the $3d_{xz}$ and $3d_{yz}$ magnetic orbitals of iron(III). Moreover, ferromagnetic contributions in a Cu(II) binuclear unit are reduced to the minimum and can be neglected whereas they must be considered for a multielectron center such as Fe(III) where

$$J = (1/n^2)\sum_{\mu\nu}J_{\mu\nu} = (2/n^2)\sum_{\mu\nu}j_{\mu\nu} + 2\Delta_{\mu\mu}\cdot S_{\mu\mu} \tag{6}$$

The ferromagnetic terms, even weak, are numerous for magnetic orbitals of different symmetries μ and ν,[41] and they can neutralize the antiferromagnetic terms $\Delta_{\mu\mu}\cdot S_{\mu\mu}$, reducing the magnitude of the antiferromagnetic coupling.

The J value of our μ-hydranilato compound is close to the reported one for the parent binuclear complex $Fe_2(dhbq)_3\cdot 4H_2O$ ($J = -2$ cm^{-1}).[34] It is worthwhile to note that such an antiferromagnetic interaction occurs between Fe(III) ions at about 7.6

(36) Julve, M.; Kahn, O. *Inorg. Chim. Acta* **1983**, *76*, L39.
(37) Wrobleski, J. T.; Brown, D. B. Unpublished results.
(38) Wrobleski, J. T.; Brown, D. B. *Inorg. Chim. Acta* **1979**, *35*, 109.
(39) (a) Michalowicz, A.; Girerd, J. J.; Goulon, J. *Inorg. Chem.* **1979**, *18*, 3004. (b) Girerd, J. J.; Kahn, O.; Verdaguer, M. *Inorg. Chem.* **1980**, *19*, 274.
(40) (a) Duggan, D. M.; Barefield, E. K.; Hendrickson, D. N. *Inorg. Chem.* **1973**, *12*, 985. (b) Battaglia, L. P.; Bianchi, A.; Corradi, A. B.; Garcia-España, E.; Micheloni, M.; Julve, M. *Inorg. Chem.* **1988**, *27*, 4174. (c) Ribas, J.; Monfort, M.; Diaz, C.; Solans, X. *An. Quim.* **1988**, *84B*, 186. (d) Bencini, A.; Bianchi, A.; Garcia-España, E.; Jeannin, Y.; Julve, M.; Marcelino, V.; Philoche-Levisalles, M. *Inorg. Chem.* **1990**, *29*, 963.
(41) (a) Girerd, J. J.; Charlot, M. F.; Kahn, O. *Mol. Phys.* **1977**, *34*, 1063. (b) Charlot, M. F.; Girerd, J. J.; Kahn, O. *Phys. Status Solidi B* **1978**, *86*, 497.
(42) The value of $J_{Cu\text{-}Cu}$ has been obtained from ref 5c, and $J_{Fe\text{-}Fe}$, from this work.

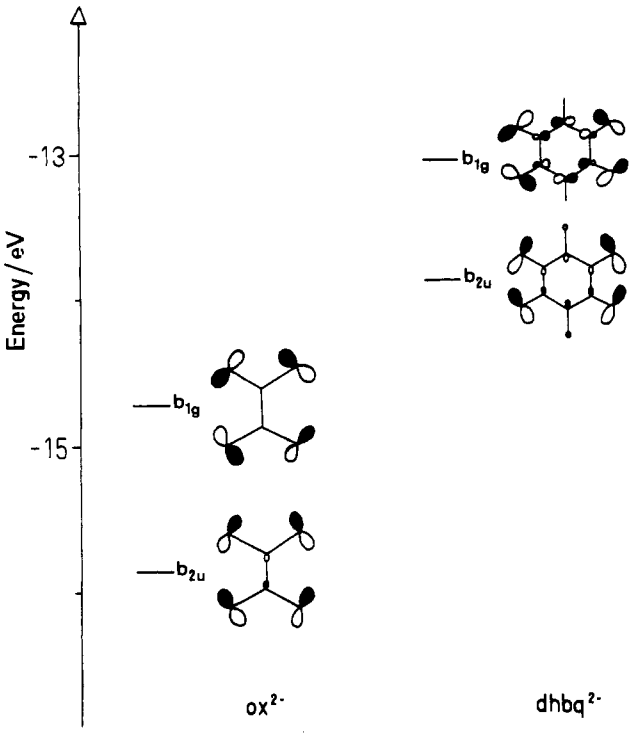

Figure 6. Schematic representation of the energies of the two HOMO's of b_{1g} and b_{2u} symmetries for oxalate and hydranilate dianions.

Å.[43] The value of n^2J for our (μ-hydranilato)iron(III) binuclear compound and that of the corresponding copper(II) binuclear complex ($J = -20.9$ cm^{-1})[9] are much closer than in the case of the oxalato bridge. This better agreement is due to the observed decrease of the ferromagnetic contributions when bridges that are more and more extended are used. The magnetic exchange in **2** can be explained in terms of molecular orbitals. The two $3d_{xy}$ magnetic orbitals of the metal ions are favorably oriented to interact on either side of the bridge, and on the other hand the two HOMO's of b_{1g} and b_{2u} symmetries (see Figure 6) are largely delocalized toward the oxygen atoms of the bridge with an orientation of the 2p oxygen orbitals that favors the overlap with the in-phase and out-of-phase combination of $3d_{xy}$ metal orbitals.

Finally, it is possible to rationalize in the same way the decrease of the exchange interaction when oxalato is substituted by hydranilato. The energy diagram depicted in Figure 6, which has been derived from extended Hückel calculations,[44] shows that the HOMO's b_{1g} and b_{2u} of oxalate are lower in energy than the corresponding ones of hydranilate. Therefore, a smaller interaction of the $3d_{xy}$ metal orbitals with the HOMO's b_{1g} and b_{2u} of oxalate is expected, which would lead to a weaker coupling. The opposite trend is experimentally observed. The larger distances O–O and Fe–Fe (about 5 and 7.6 Å for **1** and **2**, respectively) balance the tendency to a more important delocalization of the spin in **2**, leading to a weaker coupling in this case. The different coordination of the bridging ligand (bismonodentate for squarate and bisbidentate for oxalate and hydranilate) toward the metal ion leads to two different conformations of salen ligand:cis-β configuration for **1** and **2** and the stepped one for **3**. The weak coupling observed in **3** can be understood on the basis of the poor overlapping through the squarato bridge between the $dx^2 - y^2$ magnetic orbitals that are centered on each metal ion. In this regard, evidence for weak coupling has been reported very recently in 1,3-bismonodentate squarate binuclear copper(II) complexes.[32]

Conclusion

We have demonstrated the special efficiency of oxalate to transmit antiferromagnetic coupling between Fe(III) ions separated by more than 5 Å. We have proposed an upper limit of $J = -0.92$ and -0.39 cm^{-1} when oxalate is substituted by hydranilate and squarate, respectively. The exchange pathway is analyzed in terms of a simple molecular orbital model and illustrated by means of extended Hückel calculations. Unfortunately, the different coordination mode of squarate toward iron(III), when compared to the coordination of the related oxalate and hydranilate compounds, precludes a thorough rationalization of the variation of the J values through the bridges oxalate, squarate, and hydranilate in the herein reported series of binuclear iron(III) complexes.

Acknowledgment. This work was partially supported by the Comisiôn Interministerial de Ciencia y Tecnologia (Proyecto PB88-0490). Thanks are due to Dr. I. Nebot for his assistance in Hückel calculations and computing facilities and to Dr. M. Philoche for her help with structural stereodrawings.

Supplementary Material Available: Tables of crystallographic and structure refinement data (Table SI), thermal parameters (Table SII), hydrogen coordinates (Table SIII), nonessential bond lengths and angles (Table SIV), bond distances and angles involving hydrogen atoms (Table SV), and least-squares planes (Table SVI) (7 pages); a listing of observed and calculated structure factors (Table SVII) (13 pages). Ordering information is given on any current masthead page. Listings of experimental magnetic data are available from the authors on request.

(43) This distance has been computed by taking into account the crystallographic data of (μ-hydranilato)copper(II) and -nickel(II) complexes.

(44) The extended Hückel calculations were performed with the FORTICON 8 program from the Quantum Chemistry Program Exchange, with method 2 (charge iteration on all atoms). The VSIE parameters for C, O, and H and the exponents of the atomic orbitals were taken from: (a) Burns, G. J. *Chem. Phys.* **1964**, *41*, 1521. (b) Hay, P. J.; Thibeault, J. C.; Hoffmann, R. *J. Am. Chem. Soc.* **1975**, *97*, 4884.